Journal of Computational Physics 321 (2016) 892–907

Contents lists available at ScienceDirect

Journal of Computational Physics

www.elsevier.com/locate/jcp

Delayed Over-Relaxation for iterative methods

M. Antuono [a,*], G. Colicchio [a,b]

[a] CNR-INSEAN, Marine Technology Research Institute, Rome, Italy
[b] AMOS, Marine Technology Department, NTNU, Trondheim, Norway

ARTICLE INFO

Article history:
Received 29 July 2015
Received in revised form 6 June 2016
Accepted 8 June 2016
Available online 11 June 2016

Keywords:
Iterative methods
Over relaxation
Stability
Elliptic partial differential equations
Poisson equation

ABSTRACT

We propose a variant of the relaxation step used in the most widespread iterative methods (e.g. Jacobi Over-Relaxation, Successive Over-Relaxation) which combines the iteration at the predicted step, namely $(n+1)$, with the iteration at step $(n-1)$. We provide a theoretical analysis of the proposed algorithm by applying such a delayed relaxation step to a generic (convergent) iterative scheme. We prove that, under proper assumptions, this significantly improves the convergence rate of the initial iterative method. As a relevant example, we apply the proposed algorithm to the solution of the Poisson equation, highlighting the advantages in comparison with classical iterative models.

1. Introduction

The numerical modelling of physical field problems implies the rewriting of the physical equations in a discrete form, that inevitably leads to a set of linear algebraic equations. For example, heat-transfer, electrostatics, astrophysical and fluid dynamics problems are based on the numerical discretization of elliptic partial differential equations. With respect to this, iterative methods are a valid alternative to direct method (e.g. Gauss Elimination, LU decomposition) when the numerical discretization of the problems leads to large matrices. In fact, if the matrix is dense and has order N, the number of operations of a direct method is $\mathcal{O}(N^3)$ while, generally, an iterative method requires $\mathcal{O}(N^2)/\mathcal{O}(N^{3/2})$ operations. Hence, any iterative method is competitive if the number of iterations grows sublinearly with N. Even in presence of sparse matrices, direct methods may suffer from a reduced efficiency because of the fill-in phenomenon.

Iterative schemes may be roughly divided in two groups: projection methods and basic iterative methods. The former schemes rely on a projection process for extracting an approximation to the solution from a proper subspace. Some examples are the conjugate gradient (CG) or Generalized Minimal Residual (GMRES) methods which are both based on the use of the Krylov subspace (see [1,2] for details).

These schemes are quite robust but require the use of effective pre-conditioners (see, for example, [3,4]). The main limit of this kind of methods is their application to adaptively refined meshes (AMR hereinafter) if the multigrid is not used to enhance the convergence velocity through a V-cycle (e.g. [5]). In this context [6] and [7] show two different approaches for the solution of the elliptic equations. The former assembles the sparse matrix system accurately discretizing the elliptic operator in the vicinity of fine/coarse grid interfaces (assuring a reliable and accurate result), the latter combines the standard fast solvers on uniform grid and potential theory to obtain an iterative approach that preserves the order of accuracy of the uniform grid solver (assuring a faster convergence to the solutions). The disadvantage of the former is its

* Corresponding author. Tel.: +39 06 50 299 339; fax: +39 06 50 70 619.
E-mail addresses: matteo.antuono@cnr.it (M. Antuono), giuseppina.colicchio@cnr.it (G. Colicchio).

http://dx.doi.org/10.1016/j.jcp.2016.06.016
0021-9991/

cumbersome application to meshes with several areas of refinement and with dynamic mesh refinement, the latter can be characterized by small discontinuities of the first order derivatives of the solution.

The group of basic iterative methods includes, for example, the Richardson's method, Jacobi and Gauss–Seidel methods. These rely on a proper rearrangement of the initial matrix to obtain a fixed-point-like algorithm that converges to the desired solution. Their convergence is rarely guaranteed for all matrices, but a large body of theory exists for the case where the coefficient matrix arises from the finite difference discretization of elliptic partial differential equations. Despite the attractive simplicity of these methods, their convergence may be quite slow. For this reason, an over-relaxation step is often added after each cycle of the iteration to accelerate the convergence. This leads to a family of iterative methods that includes, among many others, the so-called JOR (Jacobi Over-Relaxation), SOR (Successive Over-Relaxation) and SSOR (Symmetric Successive Over-Relaxation). An exhaustive and clear description of these methods can be found in [1,2].

The aim of the present work is to give a further contribution in this direction by defining a variant of the relaxation step usually adopted in these schemes. The proposed relaxation step combines the iteration at the predicted step, namely $(n+1)$, with the iteration at step $(n-1)$ and generally leads to a significant improvement of the convergence velocity. In the following sections, we provide both a theoretical analysis and a numerical validation of the algorithm. For the sake of the simplicity, all the details of analytic results have been reported in a dedicated appendix.

2. Delayed Over Relaxation

We look for the solution of the following linear system:

$$A\,x = b\,, \tag{1}$$

where A is a $(N \times N)$ real matrix, b is real N-vector and x is the vector of unknowns. To solve the system (1), several iterative schemes may be adopted (e.g., Richardson's method, Jacobi, Gauss–Seidel, just to cite the most widespread). These may all be cast in the following general form:

$$x_{n+1} = G\,x_n + f\,, \tag{2}$$

where x_n is the n-th iterate while the matrix G and the vector f are obtained from A and b so that the scheme is convergent. This latter condition is satisfied if the spectral radius of the matrix G, hereinafter $\rho(G)$, is smaller than unity. The smaller $\rho(G)$, the faster the convergence of the scheme. To improve the convergence rate, a relaxation step is often applied after each iteration of (2):

$$\begin{cases} x^*_{n+1} = G\,x_n + f\,, \\ x_{n+1} = \omega\,x^*_{n+1} + (1-\omega)\,x_n\,, \end{cases} \tag{3}$$

where ω is the so-called relaxation parameter. This is done, for example, after the Jacobi iteration, leading to the so-called JOR method (Jacobi Over-Relaxation). A slightly different approach, used in combination with the Gauss–Seidel method, is at the basis of SOR (namely, Successive Over-Relaxation). Many variants of the latter scheme exist (e.g., backward SOR, SSOR, etc.), but they all rely on a similar procedure. The interested readers may found a deeper and sound description of these iterative algorithms in [1,2] while a brief and concise reference to JOR and SOR is provided in the Appendix B.

The main idea at the basis of the present work is to modify the relaxation step of system (3) as follows:

$$\begin{cases} x^*_{n+1} = G\,x_n + f\,, \\ x_{n+1} = \omega\,x^*_{n+1} + (1-\omega)\,x_{n-1}\,. \end{cases} \tag{4}$$

System (4) shows strong analogies with the JOR scheme but it is substantially different. In fact, its principal characteristic is the use of the iteration at step $(n-1)$ while the system (3) takes into account only the iteration at step n. For these reasons, we refer to the second equation in (4) as the Delayed Over-Relaxation step and to system (4) as the Delayed Over-Relaxation scheme. For the sake of simplicity, we denote them respectively through DOR step and DOR scheme. We prove that the model in (4) is convergent and that its convergence rate is faster than the original scheme, if G has real eigenvalues and $\omega \in (1,2)$, at the cost of an extra $1/5, 1/7$ or $1/9$ of memory allowance in one, two or three dimensions respectively when G is written in a compact form.[1]

Before proceeding to the analysis, we give a qualitative comparison between the DOR and JOR scheme. Let us denote through $e_n = (x_n - x)$ the error at the n-th iteration where x indicates the solution of system (2), namely:

$$x = G\,x + f\,. \tag{5}$$

Using the above equation, we can rearrange systems (3) and (4) as follows:

$$\begin{cases} e^*_n = G\,e_{n-1}\,, \\ e^{jor}_n = e_{n-1} + \omega\left(e^*_n - e_{n-1}\right) \end{cases} \qquad \begin{cases} e^*_{n+1} = G\,e_n\,, \\ e^{dor}_{n+1} = e_{n-1} + \omega\left(e^*_{n+1} - e_{n-1}\right) \end{cases}$$

[1] The compact form of the matrix G is necessary to reduce the memory cost from $\mathcal{O}(N^2)$ to $\mathcal{O}(N)$.

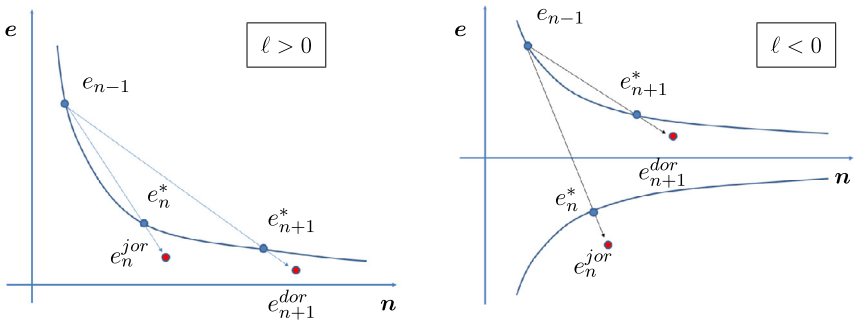

Fig. 1. Qualitative behaviour of the JOR and DOR schemes for a positive (left panel) and negative (right panel) eigenvalue ℓ of the matrix G. The horizontal and vertical axes indicate the iteration and a generic error component respectively.

This shows that the idea at the basis of the relaxation step is to modify the current iterate by using the "direction" $(e_n^* - e_{n-1})$ (JOR scheme) or $(e_{n+1}^* - e_{n-1})$ (DOR scheme). Without any loss of generality, we assume that the error vector corresponds to an eigenvector of the matrix G with (real) eigenvalue ℓ. Hence, we rewrite the above schemes as follows:

$$\begin{cases} e_n^* = \ell\, e_{n-1} \\ e_n^{jor} = e_{n-1} + \omega\left(e_n^* - e_{n-1}\right) \end{cases} \qquad \begin{cases} e_{n+1}^* = \ell\, e_n \\ e_{n+1}^{dor} = e_{n-1} + \omega\left(e_{n+1}^* - e_{n-1}\right) \end{cases}.$$

We assume $\omega > 1$ (over-relaxation) and $|\ell| < 1$ (convergence). Further, we assume that ω is chosen in such a way that each component of the vectors e_n^{jor} and e_{n+1}^{dor} has the same sign of the corresponding component of e_n^* and e_{n+1}^* respectively. This choice is always possible by continuity since $e_n^{jor} = e_n^*$ and $e_{n+1}^{dor} = e_{n+1}^*$ for $\omega = 1$. Fig. 1 schematically describes the behaviour of a generic component of the error for the iterative schemes under consideration. The dots indicate the actual values of the error while the solid lines represent its qualitative evolution. If $\ell > 0$, e_{n-1}, e_n^* and e_{n+1}^* have the same sign and, under proper conditions on ω, both schemes predict a relaxation step in the direction that reduces the magnitude of the error. On the contrary, for $\ell < 0$, e_n^* and e_{n-1} have opposite signs while e_{n+1}^* and e_{n-1} have the same sign. In this case, the step of the DOR scheme is more effective in reducing the magnitude of the error (see, for example, the right panel of Fig. 1). This qualitatively motivates the fact that the proposed scheme works properly with an over-relaxation step (i.e. for $\omega \geq 1$) while the JOR scheme is generally implemented with $\omega \leq 1$ (under relaxation).

In the following section we summarize the theoretical results on the DOR scheme. The detailed demonstrations may be found in the appendices.

2.1. Convergence of the DOR scheme

We first compute the eigenvalues of the DOR scheme defined in equation (4). This corresponds to write:

$$\begin{pmatrix} \omega G & (1-\omega)\mathbb{1} \\ \mathbb{1} & 0 \end{pmatrix} \begin{pmatrix} \phi \\ \psi \end{pmatrix} = \lambda \begin{pmatrix} \phi \\ \psi \end{pmatrix}, \tag{6}$$

where λ is an eigenvalue of the DOR scheme while ϕ and ψ are the components of the corresponding eigenvector. The above equation can be cast in the following form:

$$G\phi = \left(\frac{\lambda^2 + (\omega - 1)}{\omega\,\lambda}\right)\phi, \tag{7}$$

which indicates that ϕ is an eigenvector of the matrix G. Denoting by ℓ the eigenvalue of G associated with ϕ, we obtain the following polynomial equation:

$$\lambda^2 - \omega\,\ell\,\lambda + (\omega - 1) = 0, \tag{8}$$

which predicts two solutions in the form:

$$\lambda^{\pm}(\ell) = \frac{\omega\,\ell}{2} \pm \frac{1}{2}\sqrt{\omega^2\,\ell^2 - 4\,(\omega - 1)} \tag{9}$$

For the sake of simplicity, we reshape the DOR scheme in the following matricial form:

$$y_{n+1} = M\, y_n + \tilde{f}, \tag{10}$$

where $y_n = (x_n, x_{n-1})$, $\tilde{f} = (f, 0)$ and M is the matrix defined in equation (6).

Before proceeding to the analysis, it is interesting to compare the action of the JOR and DOR relaxation steps on the initial system in (2). This is shown in Fig. 2. The black circle represents the complex domain where $|\ell| < 1$, that is, the

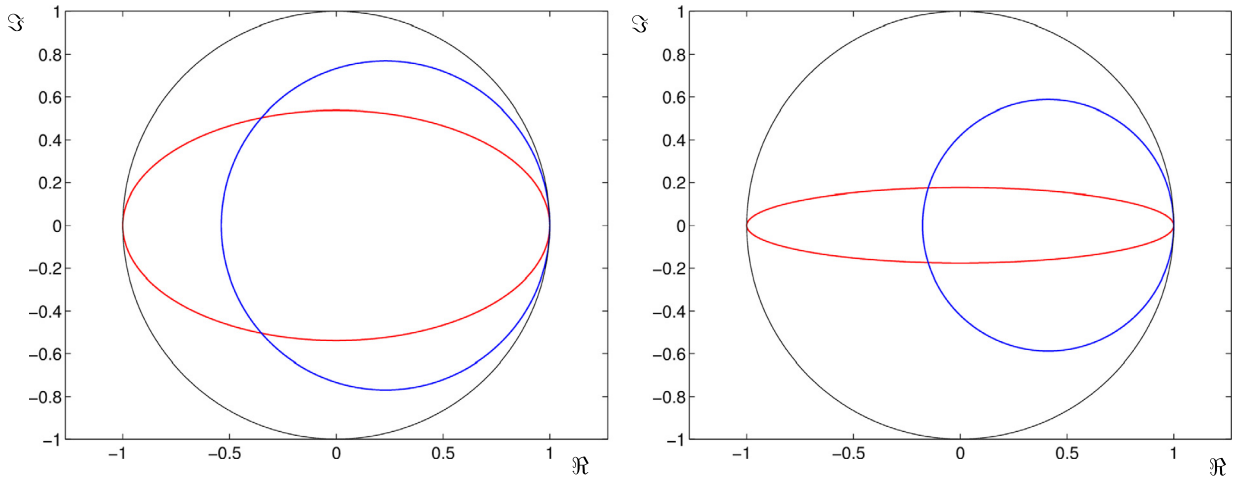

Fig. 2. Regions of stability of the JOR (blue lines) and the DOR (red lines) for $\omega = 1.3$ (left panel) and $\omega = 1.7$ (right panel). The black circle represents the region where $|\ell| < 1$, symbols $\Re$ and $\Im$ respectively indicate the real and imaginary axes. (For interpretation of the references to colour in this figure legend, the reader is referred to the web version of this article.)

region where the system in (2) is stable and convergent. The addition of an over-relaxation step shrinks the stability domain in the blue regions (JOR) and in the red regions (DOR) respectively ($\omega = 1.3$ in the left panel, $\omega = 1.7$ in the right panel). The area of these regions reduces as the relaxation parameter increases: the DOR area tends to contract along the real axis while the JOR region maintains circular but reduces its radius and translates in the direction of the positive real axis. In any case, the DOR scheme is always stable along the real axis while the JOR always shows an interval of instability along the negative semi-axis. Such a behaviour is consistent with the qualitative comparison described in Fig. 1 under the hypothesis of real eigenvalues.

Now, let us assume that the scheme in (2) is convergent. Then, the following general result holds true:

Proposition 1. *If $\rho(G) < 1$, a sufficient condition for the convergence of the DOR scheme is*

$$0 < \omega < \frac{2}{1 + \rho(G)}. \tag{11}$$

The convergence condition described in Proposition 1 is of great generality and shows that the delayed over-relaxation step has a wide range of applicability. In any case, it is overly restrictive and it does not guarantee that the DOR scheme is faster than the original iterative method. In fact, this may be false if $\Im(\ell) > \Re(\ell)$. Conversely, the DOR scheme is significantly faster than the original scheme when the eigenvalues of G are all real. This is what we prove in the following Proposition.

Proposition 2. *Let us assume that G has real eigenvalues, $\rho(G) < 1$ and $\omega \in (1, 2)$. Then, $\rho(M) < 1$. Further, if $\rho(G) > \sqrt{\omega - 1}$, this implies $\rho(M) < \rho(G)$.*

Proposition 2 states that for $\omega \in (1, 2)$ the DOR scheme is always convergent provided that the initial iterative scheme is convergent and admits only real eigenvalues. Further, the modulus of the eigenvalues of G that exceed a certain threshold is reduced by the action of the DOR algorithm. This leads to a faster convergence rate in comparison to the initial scheme. In the last Proposition, we find out the optimal choice for the relaxation parameter ω.

Proposition 3. *Under the hypotheses of Proposition 2, the optimal convergence rate of the DOR scheme is achieved for:*

$$\omega = \frac{2}{1 + \sqrt{1 - \rho(G)^2}}. \tag{12}$$

The spectral radius is $\rho(M) = \sqrt{\omega - 1}$.

The requirement for real eigenvalues is surely satisfied if G is symmetric. In any case, this does not compete the range of applications for the DOR. In fact, there exist some relevant physical problems that are characterized by differential operators with real eigenvalues. The discrete representation of such operators is generally non-symmetric and admits eigenvalues with a small imaginary part. Under these conditions, the DOR scheme may still be used. This is what we show in the following section.

3. Applications

In this section we apply the proposed relaxation step to different iterative methods and show its advantages by studying the solution of elliptic problems. To this purpose, we briefly recall some results on the elliptic equations.

Let us consider the following elliptic differential operator:

$$L[u] = \mathrm{div}\,(h\,\mathrm{grad}(u))\,, \tag{13}$$

where u is the unknown variable and h is a positive function that may represent a physical density or a metric term (e.g. the Laplacian in polar coordinates). Each eigenvalue λ of L is obtained by solving the following problem:

$$L[\phi] = \lambda\,\phi\,, \tag{14}$$

where ϕ is the related eigenvector and null boundary conditions (Dirichlet, Neumann or mixed) are imposed along $\partial\Omega$ (here Ω denotes the problem domain). Working through the equations and using the boundary conditions, it is possible to rearrange (14) as follows:

$$\lambda = -\frac{\displaystyle\int_\Omega h\,\|\mathrm{grad}(\phi)\|^2\,\mathrm{d}V}{\displaystyle\int_\Omega \phi^2\,\mathrm{d}V}\,. \tag{15}$$

The above equation confirms that the eigenvalues of (13) are real (negative) and suggests that the DOR relaxation step may be fruitfully used to solve the corresponding discrete problem, that is:

$$L[u] = f \qquad \longrightarrow \qquad A\,x = b\,. \tag{16}$$

The basic iterative schemes used for the validation of the DOR step are the Richardson's method, the Jacobi and Gauss–Seidel schemes and their over-relaxation variants JOR and SOR. All these methods are briefly described in the Appendix B. Here we just recall their iteration matrix, namely the matrix G in equation (2). First, we decompose the initial matrix as $A = D - E - F$ where D is the diagonal part and $-E$ and $-F$ are the lower and upper triangular matrices respectively. Then, the iteration matrices for the Richardson's method, Jacobi, Gauss–Seidel and SOR are:

$$G_{rich} = \mathbb{1} + \Delta\tau\,A\,, \qquad G_{jac} = D^{-1}\,(E+F)\,,$$
$$G_{GS} = (D-E)^{-1}\,F\,, \qquad G_{SOR} = (D-\omega\,E)^{-1}\,[\,\omega\,F + (1-\omega)\,D\,]\,.$$

Note that the Richardson's method (here we implement its simplest form) already relies on the use of a relaxation-type parameter, namely $\Delta\tau$. Hereinafter, this is referred to as the pseudo-time parameter (see the Appendix B for details). Incidentally, we highlight that the Richardson's method can be generalized to include a wide family of basic iterative solvers and that Jacobi, Gauss–Seidel, JOR and SOR can be regarded as specific forms of such a generalized scheme (see [1,2] for details). As explained in the previous section, the JOR method is obtained by applying the iteration step to the Jacobi scheme. Finally, we underline that the iteration matrix for SOR depends implicitly on ω.

According to [1,2], the iterations are stopped when the L_2-norm of the residue is smaller than a threshold value, namely:

$$\|r_n\| \le \delta_r\,\|r_0\|\,, \tag{17}$$

where $r_n = Ax_n - b$ is the residue of the n-th iteration and $r_0 = Ax_0 - b$ is the initial residue. In all the simulations, we set $\delta_r = 10^{-12}$ and chose $x_0 = 0$ as initial guess.

3.1. The Taylor–Green vortex

The Taylor–Green vortex is an analytic solution of the two-dimensional Navier–Stokes equations which is periodic in space and strictly decaying in time (for details see [8]). The pressure field is obtained from the solution of the Poisson equation and it is used as comparison between different iterative schemes. As shown in Fig. 3, a squared domain $\mathcal{D} = [-\pi/4, 7\pi/4] \times [-\pi/4, 7\pi/4]$ has been considered. The (dimensionless) pressure field solution at time t is:

$$p = \frac{1}{4}\,[\,\cos(2x) + \cos(2y)\,]\,e^{-\frac{4}{Re}t}\,, \tag{18}$$

where Re is the Reynolds number. The pressure solution obeys to the following Poisson equation:

$$\Delta p = -\,[\,\cos(2x) + \cos(2y)\,]\,e^{-\frac{4}{Re}t}\,. \tag{19}$$

The Dirichlet and Neumann boundary conditions are calculated by using equation (18). Since we are not dealing with dynamic problems, we just consider the solution at $t = 0$.

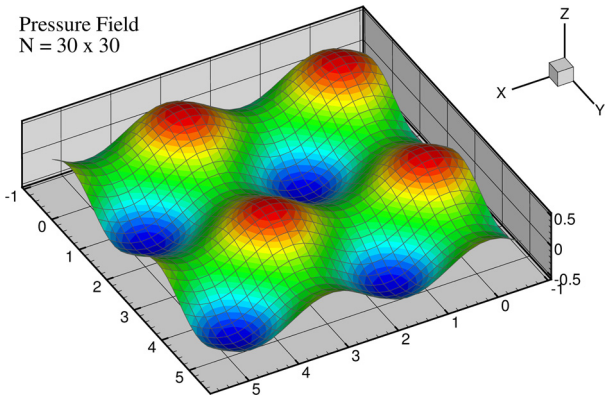

Fig. 3. Sketch of the (dimensionless) Taylor–Green solution for the pressure field at the initial time $t = 0$.

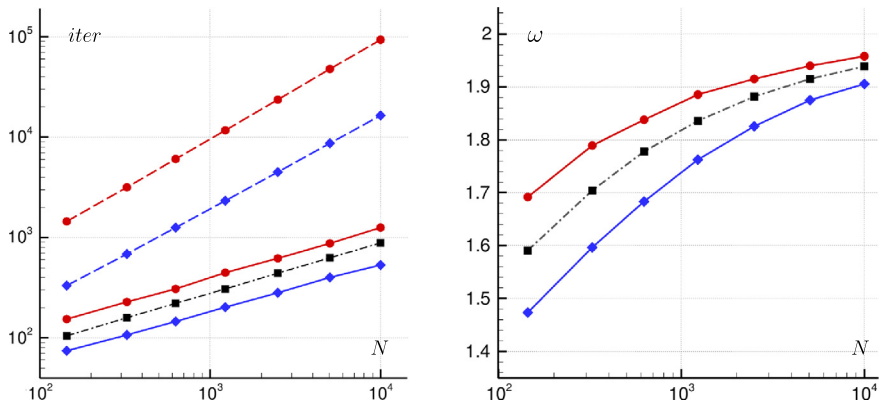

Fig. 4. The Taylor–Green vortex. Left panel: iterations to reach the convergence for number of grid points. Dashed lines indicate the Richardson method, the solid lines denote the same scheme with the addition of the DOR relaxation step while the dot-dashed line represents the expected iterations for the latter scheme according to Proposition 3. Symbols ⋄ and ∘ respectively indicate the Dirichlet and Neumann conditions. Right panel: the relaxation parameter as function of the grid points. The dot-dashed line indicates the theoretical values of ω computed according to Proposition 3.

3.1.1. Comparison with basic iterative methods

The Poisson equation is discretized by central finite difference to the second-order accuracy. A uniform Cartesian grid is adopted and seven resolutions are used, namely $N = 12 \times 12, 18 \times 18, 25 \times 25, 35 \times 35, 50 \times 50, 71 \times 71$ and 100×100 grid points. A sketch of the pressure solution at $t = 0$ is drawn in Fig. 3. Both Neumann and Dirichlet boundary conditions have been enforced. Since the JOR scheme is always divergent for $\omega > 1$ while it is slower than the Jacobi scheme for $\omega \leq 1$, it has not been considered for comparison.

Fig. 4 (left panel) shows the effects of the DOR relaxation step on the Richardson's method. The same behaviour is obtained for the Jacobi method which, therefore, is not shown here. The eigenvalues of the initial matrix A have been estimated by using the theoretical results reported in the Appendix B.1, these holding true for the Laplacian operator discretized on a uniform Cartesian grid in the presence of Dirichlet conditions. This allowed for the computation of the spectral radius of the iteration matrix, of the optimal pseudo-time parameter $\Delta\tau$ and, for the DOR variant, of the optimal relaxation parameter ω (see the Proposition 3). In Fig. 4, the theoretical values of ω and the corresponding expected number of iterations are displayed through dot-dashed lines. Because of the approximations in the estimation of spectral radius, the optimal convergence rate for the DOR variant has been obtained by slightly varying ω in the neighbourhood of the theoretical values. In particular, the Neumann and Dirichlet assignment lead to different results because the matrix A is slightly different for these two conditions. The discrepancy between the theoretical and numerical optimal values of ω reduces as N increases, since the estimates in the Appendix B become more and more accurate. The convergence scaling, namely $\alpha = \log(\#iterations)/\log(N)$, is about 1.1 and 1.3 for the Richardson's method with Dirichlet and Neumann conditions respectively and 0.75 and 0.87 for the DOR variant.

Fig. 5 (left and middle panels) displays the theoretical and numerical convergence rates of the Richardson's method and of its relaxation variant. The numerical convergence rate is defined as $\sigma_n = -\log(\|r_{n+1}\|/\|r_n\|)$ while the theoretical one is given by $\sigma = -\log(\rho(G))$ (here log indicates the natural logarithm). For the Richardson's method the numerical convergence rate is always larger than the theoretical one (which is about $3.812 \cdot 10^{-3}$) and for n large tends to $9.544 \cdot 10^{-3}$. Such a discrepancy is due to the fact that, in this specific test case, the initial residue of the Richardson's method does not contain components along the direction of the eigenvector associated with the maximum absolute eigenvalue. Since the latter one is

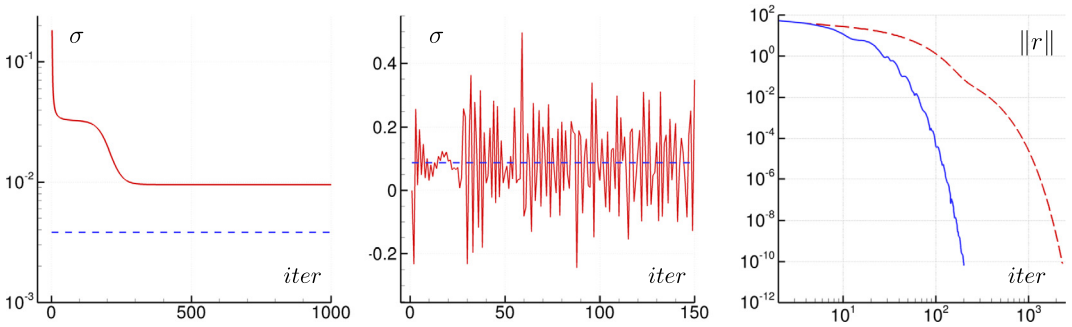

Fig. 5. Taylor–Green vortex with Dirichlet boundary conditions ($N = 35 \times 35$). Numerical (solid lines) and theoretical (dashed lines) convergence rate for the Richardson's method (left panel) and the same scheme with the addition of the DOR relaxation step (middle panel). Right panel: the evolution of the residue for the Richardson's method (dashed line) and its DOR variant (solid line).

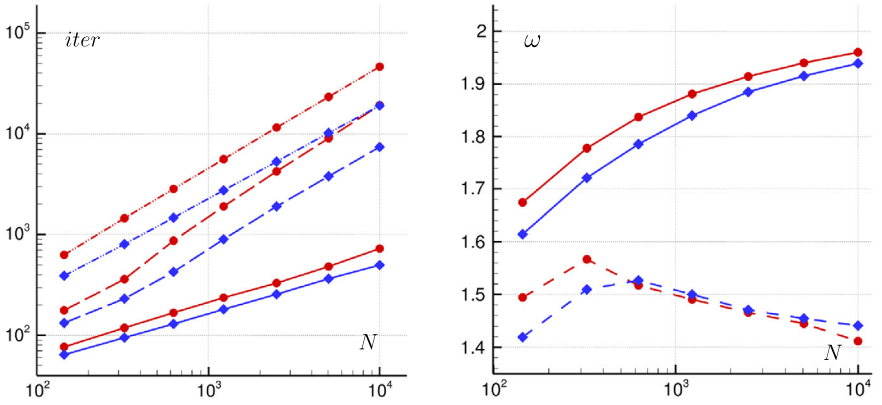

Fig. 6. The Taylor–Green vortex. Left panel: iterations to reach the convergence for number of grid points. Dot–dot-dashed lines denote the Gauss–Seidel method, dashed lines indicate the same method with the addition of the DOR relaxation step and solid lines denote the SOR scheme. Symbols ◇ and ○ respectively indicate the Dirichlet and Neumann conditions. Right panel: the relaxation parameter as function of the grid points.

related to the slowest damping rate, the numerical convergence reveals faster than the theoretical one. In the DOR variant, the theoretical convergence rate (evaluated according to the Proposition 3) is about $8.737 \cdot 10^{-2}$ and the numerical signal oscillates around this value as a consequence of the non-monotone behaviour of the residue (see the right panel of Fig. 5). This feature is qualitatively the same for all the considered cases and it is a consequence of the fact that the iteration matrix of the DOR variant admits complex eigenvalues (see the Appendix A.3) while the Richardson's one has real eigenvalues.

For both the Richardson's and Jacobi schemes the iteration matrix is symmetric and, therefore, has real eigenvalues, these representing the optimal conditions under which the DOR algorithm may work. When we consider the Gauss–Seidel method, the matrix G is no more symmetric and it may have eigenvalues with non-null complex part. This implies that the addition of the DOR step cannot ensure the convergence for all ω in $(1, 2)$ and the relaxation parameter has to be smaller than a certain threshold value as a consequence of Proposition 1. Further, there is not a clear way to find out an optimal value of ω and, therefore, this is done by attempts. In any case, the addition of the DOR step still provides a fairly good speed-up when applied to the Gauss–Seidel method, though this becomes less and less pronounced as the number of grid points increases (left panel of Fig. 6). The SOR scheme proves to be the one requiring less iterations while the Richardson's (Jacobi) methods with the DOR step require just a slightly higher number (see Fig. 4).

The right panel of Fig. 6 reports the values of ω for the SOR and for the Gauss–Seidel scheme with the DOR step. In the latter case, the behaviour of the relaxation parameter is quite different from that depicted in Fig. 4 (right panel) and is likely due to the occurrence of complex eigenvalues. Regarding the SOR with Neumann conditions, the optimal value of ω has been chosen by attempts to maximize the velocity of the scheme. Conversely, for Dirichlet conditions it has been possible to use the theoretical expression described in [1,2] (which holds true when the matrix A is tridiagonal, symmetric and positive definite). Such a theoretical formula is identical to that given in Proposition 3 but, for SOR, $\rho(G)$ has to be substituted with the spectral radius of the Jacobi matrix. Because of the absence of theoretical estimations of $\rho(G)$ for the Jacobi matrix, this has been computed numerically, leading to an increase of the computational effort.

As a final example, Fig. 7 displays the Taylor–Green vortex with Dirichlet conditions for $N = 128 \times 128, 256 \times 256, 512 \times 512$ and 1024×1014, comparing the SOR scheme and the Richardson's method with the DOR relaxation step. Remarkably, the algorithms show a similar behaviour for both the number of iterations to reach the convergence and the values of ω. Incidentally, we underline that the latter ones have been chosen by attempts for both the methods because the numeri-

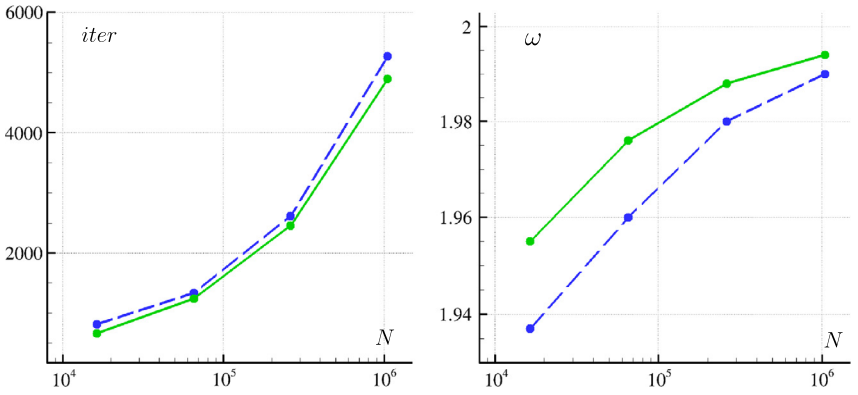

Fig. 7. The Taylor–Green vortex with Dirichlet conditions. Left panel: iterations to reach the convergence for number of grid points. Dashed lines denote Richardson's method with the DOR relaxation step and the solid lines denote the SOR scheme. Right panel: the relaxation parameter as function of the grid points.

cal evaluation of $\rho(G)$ to compute the optimal values of ω was computationally too expensive for the resolutions under examination.

From the above analysis, we can conclude that the DOR step always leads to an increase of the convergence rate of the basic iterative schemes (e.g., Richardson's, Jacobi and Gauss–Seidel methods) when the relaxation parameter is chosen in accordance with the results of Propositions 1, 2 and 3. The Richardson's method, along with the Jacobi scheme, is the iterative method requiring the highest number of iterations among those considered here. Despite this, the addition of the DOR step makes it comparable to the SOR. This has a great importance for applications. First, the Richardson's method does not require a matrix inversion. This leads to a drastic reduction of the computational costs and it makes its parallelization straightforward. Further, the matrix G likely has eigenvalues with a small imaginary part, since it directly comes from the discretization of elliptic partial differential equations. Under these conditions, the Propositions 1 and 2 ensure the convergence and the efficiency of the scheme. For these reasons, we only consider the Richardson's method with DOR step in the sequel of the present work. Hereinafter, we refer to this scheme as the DOR method.

4. The DOR method

When the DOR step is applied to the Richardson algorithm, it reads:

$$\begin{cases} x^*_{n+1} = x_n + \Delta\tau\,(A\,x_n - b)\,, \\ x_{n+1} = \omega\,x^*_{n+1} + (1-\omega)\,x_{n-1}\,. \end{cases} \tag{20}$$

The optimal values of ω and $\Delta\tau$ are obtained through the knowledge of the maximum and minimum eigenvalues of the matrix A and by using the Proposition 3 and the results of Appendix B. In practice, the evaluation of the eigenvalues can be very time consuming and small variations of the values of ω and $\Delta\tau$ may strongly influence the convergence rate of the scheme.

Different strategies may be adopted to overcome this issue, e.g. the Steepest Descent, the Minimal Residual and the Residual Norm Steepest Descent algorithms, just to cite the most widespread. In their basic formulation (see [1,2]), such algorithms can be applied to the Richardson's method straightforwardly and rely on an appropriate adjustment of the relaxation parameter during the iterations in order to increase the convergence rate.

Here, we extend the Minimal Residual algorithm to the couple $(\Delta\tau, \omega)$ in order to minimize the residue of the n-th iteration. While the use of such a method for the estimation of $\Delta\tau$ is quite well-known, its application to the parameter ω is proposed here for the first time. On the contrary, it will not be applied to the SOR scheme since its iteration matrix depends on the relaxation parameter implicitly, making its computational cost prohibitive.

4.1. Minimal Residual DOR method

The implementation of the Minimal Residual algorithm to the DOR method may be done in two different ways. One is obtained by finding the local minimum of the residue $\|r_{n+1}\|$ in the $(\Delta\tau, \omega)$-plane. It is possible to prove that only two extrema exist (a saddle point and a local minimum) but we could not prove that the local minimum is a global one. Apart from this, such a scheme does not provide a net improvement with respect to the basic DOR scheme (i.e., that described in section 3.1.1). Further, the values of $\Delta\tau_n$ and ω_n show large oscillations and, sometimes, cross the zero. A more reliable approach is based on a successive use of $\Delta\tau_n$ to minimize $\|r^*_{n+1}\|$ and of ω_n to reduce $\|r_{n+1}\|$. This approach leads to:

$$\Delta\tau_n = -\frac{\langle r_n\,,\, A\,r_n\rangle}{\|A\,r_n\|^2}\,, \qquad \omega_n = \frac{\langle\, r_{n-1},\, r_{n-1} - r^*_{n+1}\,\rangle}{\|r_{n-1} - r^*_{n+1}\|^2}\,, \tag{21}$$

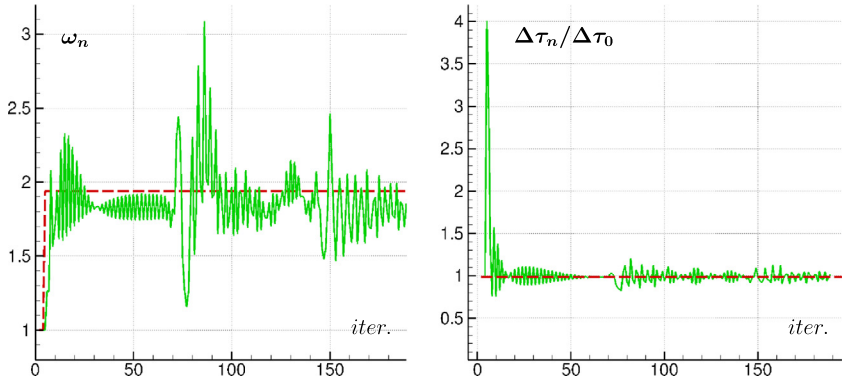

Fig. 8. Taylor–Green with $N = 100 \times 100$ and Dirichlet boundary conditions. Evolution of ω_n (left) and $\Delta\tau_n$ (right) for the MR-DOR method. The dashed lines indicate the optimal values computed for the DOR method in (20).

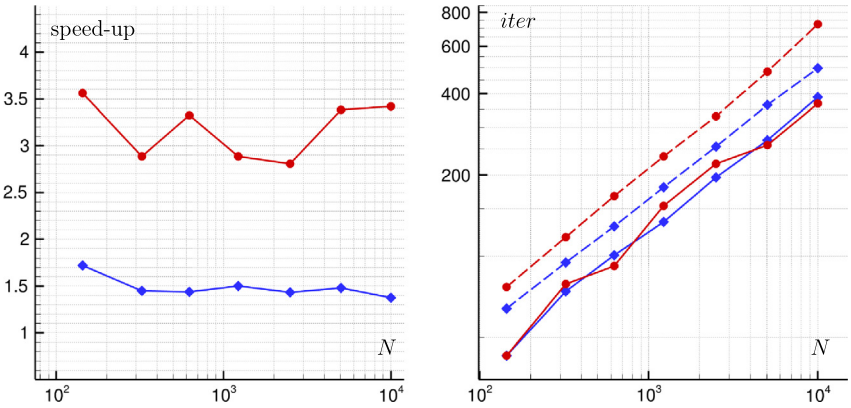

Fig. 9. The Taylor–Green vortex. Left panel: speed-up of the MR-DOR with respect to the DOR method (see Fig. 4). Symbols ⋄ and ○ respectively indicate the Dirichlet and Neumann conditions. Right panel: iterations to reach the convergence for number of grid points. The dashed lines denote the SOR scheme (same case of the left panel of Fig. 6) and the solid lines indicate the MR-DOR method.

where $r^*_{n+1} = r_n + \Delta\tau_n A r_n$. As shown in the Appendix C, $\Delta\tau_n$ and ω_n are the points of the unique global minima for $\|r^*_{n+1}\|$ and $\|r_{n+1}\|$ respectively. According to equation (15), the matrix A is negative definite (at least approximatively) and, consequently, $\Delta\tau_n$ is positive. Conversely, we failed in proving that ω_n is always positive (although we never observed negative values). In some cases, ω_n may temporarily decrease below the unity and, therefore, decelerate the convergence. To avoid such an issue, it is sufficient to modify the equation for ω_n as follows:

$$\omega_n = \max\left[\frac{\langle r_{n-1},\, r_{n-1} - r^*_{n+1}\rangle}{\|r_{n-1} - r^*_{n+1}\|^2},\, 1\right]. \tag{22}$$

Fig. 8 gives an example of the evolution of ω_n and $\Delta\tau_n$ for the Taylor–Green vortex with $N = 100 \times 100$ and Dirichlet boundary conditions. Here the dashed lines indicate the optimal values of ω and $\Delta\tau$ used for the DOR scheme. These have been computed by using the Proposition 3 and the results of Appendices B and B.1. Remarkably, both $\Delta\tau_n$ and ω_n oscillate in the neighbourhood of the optimal values and sometimes exceed them. Moreover, ω_n does not remain in the theoretical range of stability, namely $(1, 2)$. This behaviour may be caused by the necessity of eliminating some components of the residue that are associated with the eigenvalues at the boundary of the stability region. The use of an over-relaxation parameter out of the stability range has been already reported in some works and, under suitable conditions, can lead to a significant increase of the convergence rate. For example, in Yang & Mittal [9], a scheduled relaxation approach has been proposed for the parameter $\Delta\tau$, showing a large acceleration of the Richardson's method. There, the values and the sequence of the relaxation parameters have to be defined before running the simulation. Further, the method is sensitive on the truncation errors caused by round-off and arithmetical overflow. The approach proposed in (21) gives an evaluation of $\Delta\tau_n$ and ω_n during the iterations and no sensitivity on truncation errors has been observed.

The performances of the Minimal Residual DOR method (hereinafter MR-DOR) have been tested for the Taylor–Green vortex problem versus the DOR method defined in system (20). In the latter case, the results are those reported in Fig. 4. The left panel of Fig. 9 displays the speed-up (namely, the ratio between the number of iterations) induced by the residual norm steepest descent algorithm on the basic scheme. The speed-up is about 1.5 times for the Dirichlet problems while increases to about 3.3 in the presence of Neumann conditions. This is not a moderate improvement since the DOR method

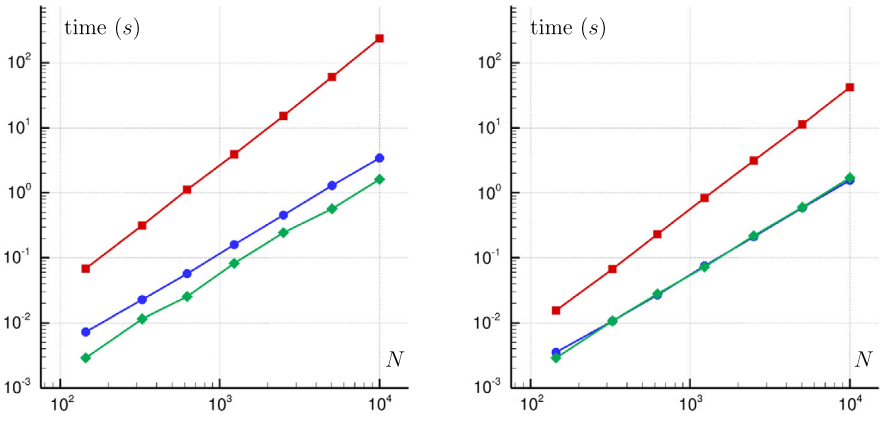

Fig. 10. The Taylor–Green vortex. The CPU time (in seconds) for Richardson's (□), DOR (○) and MR-DOR (◇) methods under Neumann (left) and Dirichlet (right) conditions.

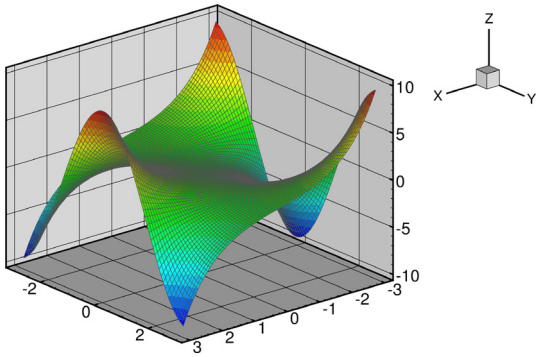

Fig. 11. Sketch of the solution ϕ of equation (23) ($N = 80 \times 80$).

has been *optimized* through a careful tuning of the parameters $(\Delta\tau, \omega)$ whose estimation is rather complex. Further, the convergence rate is generally very sensitive to small variations/approximations of them. The use of the Minimal Residual algorithm overcomes these issues and allows the definition of a robust and fast scheme.

When compared to the SOR method, as in the right panel of Fig. 9, the MR-DOR method shows a faster convergence rate. In Fig. 10 we compare the CPU times for Richardson's, DOR and MR-DOR methods. The CPU time is calculated by using a single core on an Intel Xeon(R) CPU X5650, 2.3 GHz. In the presence of Neumann conditions, the MR-DOR is about twice faster than the DOR method while they are practically equivalent when Dirichlet conditions are implemented. In fact, in the latter case the increase in the convergence rate is compensated by the increase in the computational operations for the dynamical evaluation of $\Delta\tau_n$ and ω_n. Apart from these considerations, the MR-DOR scheme is always preferable since it provides an "optimized" scheme without any tuning of parameters. Further, it proves to be useful in all those problems in which the estimation of the optimal values of $\Delta\tau$ and ω is difficult or practically impossible. This is shown in the next sections.

4.2. A test case with non-uniform density

In this section we consider the following elliptic problem in Cartesian coordinates:

$$\nabla \cdot (h \nabla \phi) = b\,, \tag{23}$$

where h represents a non-uniform "density". Specifically, we chose:

$$h = 2 + \tanh(x)\,, \qquad b = \frac{\cos(y)}{\cosh(x)}\,, \qquad \phi = \sinh(x)\cos(y)\,. \tag{24}$$

A sketch of the solution ϕ is depicted in Fig. 11 in a domain $\mathcal{D} = [-3, 3] \times [-3, 3]$ for $N = 80 \times 80$. Because of the presence of h, it is not possible to use the estimates of the eigenvalues described in Section B.1 and, consequently, the evaluation of the optimal values for $\Delta\tau$ and ω becomes prohibitive. Under these conditions, the use of the MR-DOR scheme turns out to be particularly convenient.

Fig. 12 shows the iterations necessary for convergence with: *a*) the Richardson's method with the Minimal Residual algorithm, hereinafter MR-Richardson [$\Delta\tau_n$ is obtained as in (21)], *b*) the SOR scheme (with a properly tuned relaxation

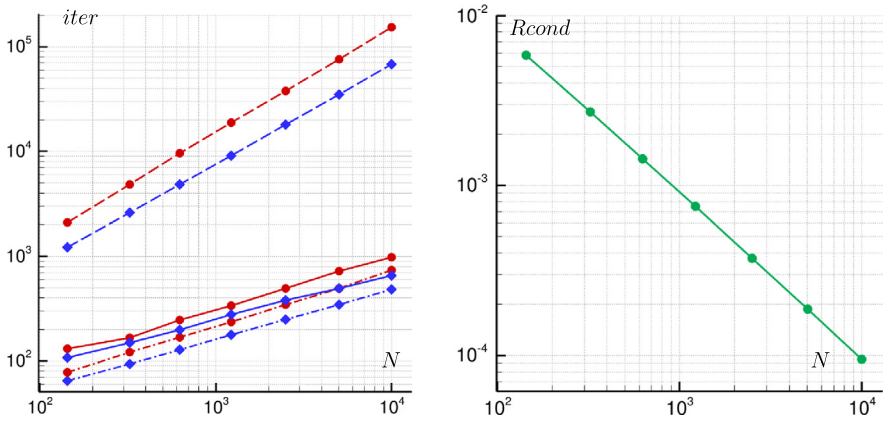

Fig. 12. Problem with non-uniform density. Left panel: iterations to reach the convergence for the MR-Richardson method (dashed lines), SOR (dot-dashed lines) and MR-DOR (solid lines). The symbol ∘ stands for Neumann conditions while ◇ for Dirichlet conditions. Right panel: the reciprocal condition number in L_1-norm of the matrix A with Dirichlet conditions.

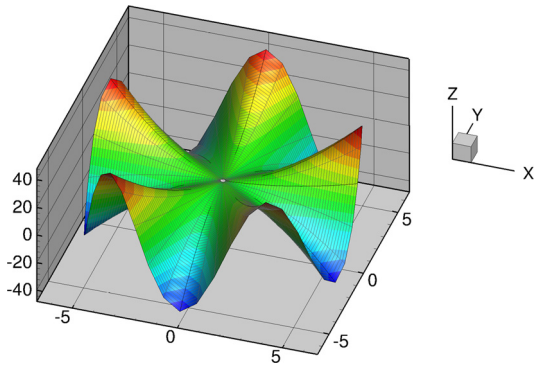

Fig. 13. Sketch of the solution $\phi = r^2 \sin(5\theta)$ in polar coordinates ($N = 50 \times 50$).

parameter ω) and c) the MR-DOR. As displayed in the left panel of Fig. 12, the MR-DOR requires a slightly higher number of iterations than SOR while it is much faster than the MR-Richardson's method. In the latter case, the speed-up for $N = 100 \times 100$ is about 100 for Dirichlet conditions and 150 for Neumann conditions. This further confirms that the speed-up of the MR-DOR is mainly due to the application of the Minimal Residual algorithm to ω rather than $\Delta\tau$. The right panel of the same figure shows the reciprocal condition number of the matrix A with Dirichlet boundary conditions, namely:

$$Rcond = \left(\|A\|_1 \, \|A^{-1}\|_1 \right)^{-1}, \tag{25}$$

where $\|\cdot\|_1$ denotes the L_1-norm. This gives an idea of the effect of the increase of N on the conditioning of the matrix.

4.3. A test case in polar coordinates

To complete the analysis of the DOR method, we study the solution of the Poisson equation in polar coordinates. As usual, we denote through r and θ the radial and angular coordinates. The problem under consideration is represented by the equation below:

$$\frac{1}{r}\frac{\partial}{\partial r}\left(r \frac{\partial \phi}{\partial r} \right) + \frac{1}{r^2}\frac{\partial^2 \phi}{\partial \theta^2} = b\,, \tag{26}$$

which has been discretized by second-order finite difference as described in [10]. In particular, we choose:

$$\phi(r,\theta) = r^2 \sin(a\,\theta)\,, \qquad b(r,\theta) = (4 - a^2)\, r^2 \sin(a\,\theta)\,, \tag{27}$$

with $a = 5$. A sketch of the solution is drawn in Fig. 13 on the domain $\mathcal{D} = [-2\pi, 2\pi] \times [-2\pi, 2\pi]$ for $N = 50 \times 50$. Similarly to the case with non-uniform density, it is not possible to use the formulas of section B.1 to estimate the eigenvalues of the Laplacian and provide an approximation for $\Delta\tau$ and ω. Again, the MR-DOR model represents a simple and reliable alternative to an explicit guess on such parameters. Fig. 14 further confirms the superiority of the MR-DOR with respect to the MR-Richardson's method.

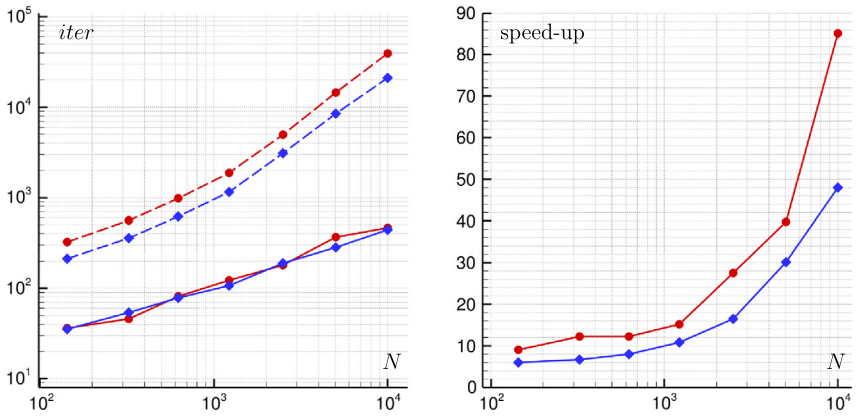

Fig. 14. Problem in polar coordinates. Left panel: iterations to reach the convergence for the MR-Richardson method (dashed lines) and the MR-DOR (solid lines). Right panel: the speed-up. The symbol ∘ stands for Neumann conditions while ⋄ for Dirichlet conditions.

5. Conclusions

We proposed a variant of the relaxation step used in the most widespread iterative methods (e.g. JOR, SOR) which combines the iteration at the predicted step, namely $(n+1)$, with the iteration at step $(n-1)$. We first provided a theoretical analysis of the proposed algorithm by applying the delayed relaxation step to a generic (convergent) iterative scheme. We proved that, under proper assumptions, this significantly improves the convergence rate of the initial iterative method. The theoretical findings were confirmed by the numerical test cases.

The use of the delayed over-relaxation step proved to be particularly convenient when applied to the classic Richardson's method. The match between the former scheme and the relaxation step can be regarded as a new model, i.e. the DOR method, that depends on two different relaxation parameters (namely $\Delta\tau$ and ω).

To improve the convergence velocity and to avoid an explicit guess of the former parameters, the DOR method has been further enhanced by applying the Minimal Residual algorithm. This approach proved to be reliable and robust and to extend the range of applicability of the DOR method to more general elliptic problems (e.g. non-uniform density, polar coordinates). A possible extension of the scheme may include multigrid approaches in the solution and its adaptation to AMR grids.

Acknowledgements

This research activity has been partially supported by the Flagship Project RITMARE – The Italian Research for the Sea – coordinated by the Italian National Research Council. It has been also partially founded by the Centre for Autonomous Marine Operations and Systems (AMOS), NTNU, Trondheim (project number 223254).

Appendix A. Details of the demonstrations

A.1. Proof of Proposition 1

If $\rho(G) < 1$, a sufficient condition for the convergence of the DOR scheme is

$$0 < \omega < \frac{2}{1 + \rho(G)}\,. \tag{A.1}$$

Proof. Let us consider the complex domain $E = \{\, z \in \mathbb{C} \,\big|\, |z| < 1 \,\}$ and split the polynomial (8) in the following way:

$$f(z) = z^2 \qquad g(z) = -\omega\,\ell\, z + (\omega - 1)\,.$$

Then, we impose the following inequality to hold true along ∂E:

$$|g(z)| \le \omega\,|\ell| + |\omega - 1| < 1 = |z^2| = |f(z)|\,. \tag{A.2}$$

The Rouchè theorem implies that the holomorphic functions f and $f+g$ have the same number of zeros in E. The latter case means that both roots of equation (8) are inside E. Consequently, $|\lambda^{\pm}(\ell)| < 1\ \forall \ell$ and this ensures that the scheme is convergent. Now, we have to find the value of ω that guarantees the fulfilment of the inequality in (A.2) for every choice of ℓ. Let us assume that $\omega \le 1$. Then, the inequality becomes:

$$\omega\,(|\ell| - 1) < 0\,, \tag{A.3}$$

that is surely satisfied for $\omega > 0$, since $|\ell| < 1$. Now, assume that $\omega > 1$. Then, the inequality becomes:

$$\omega < \frac{2}{1+|\ell|}. \tag{A.4}$$

Since this inequality has to hold true whatever is ℓ, we require:

$$\omega < \frac{2}{1+\rho(G)} \leq \frac{2}{1+|\ell|}. \tag{A.5}$$

Collecting all the above results together, we obtain the thesis. □

A.2. Proof of Proposition 2

Let us assume that G has real eigenvalues, $\rho(G) < 1$ and $\omega \in (1,2)$. Then, $\rho(M) < 1$. Further, if $\rho(G) > \sqrt{\omega-1}$, this implies $\rho(M) < \rho(G)$.

Proof. Let us consider equation (9) and assume that $\lambda^{\pm}(\ell)$ are real. This occurs when ℓ and ω satisfy the following inequality:

$$|\ell| \geq 2\frac{\sqrt{\omega-1}}{\omega}. \tag{A.6}$$

For $\omega \in (1,2)$ the lower bound is always smaller than the unity and this is consistent with the hypothesis $|\ell| < 1$. First, we prove that $|\lambda^{\pm}(\ell)| < |\ell|$. Rearranging (9), we obtain the following inequalities:

$$\begin{cases} -k_2 < \sqrt{\omega^2\ell^2 - 4(\omega-1)} < k_1 \\ -k_1 < \sqrt{\omega^2\ell^2 - 4(\omega-1)} < k_2, \end{cases} \tag{A.7}$$

where

$$k_1 = 2|\ell| + \omega\ell, \qquad k_2 = 2|\ell| - \omega\ell. \tag{A.8}$$

The hypothesis $\omega < 2$ ensures that both k_1 and k_2 are positive and, consequently, the inequalities in (A.7) simplify as follows:

$$\sqrt{\omega^2\ell^2 - 4(\omega-1)} < k_1, \qquad \sqrt{\omega^2\ell^2 - 4(\omega-1)} < k_2. \tag{A.9}$$

Squaring the above relations, we find:

$$1-\omega < \ell^2 + \omega\ell|\ell|, \qquad 1-\omega < \ell^2 - \omega\ell|\ell|, \tag{A.10}$$

which are both true for $\omega \in (1,2)$ and $|\ell| < 1$. Now assume that $\lambda^{\pm}(\ell) \in \mathbb{C}$, that is:

$$|\ell| < 2\frac{\sqrt{\omega-1}}{\omega}. \tag{A.11}$$

In this case $|\lambda^{\pm}| = \sqrt{\omega-1}$ and, for $\omega \in (1,2)$, we have $|\lambda^{\pm}| < 1$. This implies that $\rho(M) < 1$ and completes the first part of the proof. For the demonstration of the second statement, we collect all the findings as follows:

$$\lambda^{\pm} \in \mathbb{R} \quad \Rightarrow \quad \rho(M) < \rho(G)$$

$$\lambda^{\pm} \in \mathbb{C} \quad \Rightarrow \quad \begin{cases} \rho(M) < \rho(G) & \text{for} \quad \sqrt{\omega-1} < \rho(G) < 2\sqrt{\omega-1}/\omega \\ \rho(G) \leq \rho(M) & \text{for} \quad \rho(G) \leq \sqrt{\omega-1} \end{cases}$$

Then, the DOR scheme is faster than the original one if $\sqrt{\omega-1} < \rho(G)$. □

A.3. Proof of Proposition 3

Under the hypotheses of Proposition 2, the optimal convergence rate of the DOR scheme is achieved for:

$$\omega = \frac{2}{1+\sqrt{1-\rho(G)^2}}. \tag{A.12}$$

The spectral radius is $\rho(M) = \sqrt{\omega-1}$.

Proof. First we require the DOR algorithm to be faster than the original iterative scheme. Accordingly to Proposition 2, this corresponds to $\rho(G) > \sqrt{\omega-1}$. In this range, we look for the value of ω that guarantees the faster convergence of the DOR

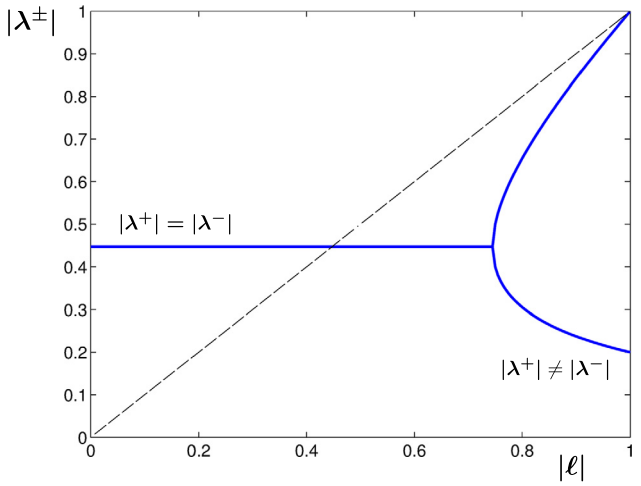

Fig. A.1. Action of the DOR scheme on the eigenvalues of the matrix G for $\omega = 1.2$. Accordingly to Proposition 2, $\max(|\lambda^{+}|, |\lambda^{-}|) < |\ell|$ for $|\ell| > \sqrt{\omega - 1}$. Further, $|\lambda^{+}| = |\lambda^{-}| = \sqrt{\omega - 1}$ in the range where $\lambda^{\pm}$ are complex (i.e. for $|\ell| < 2\sqrt{\omega - 1}/\omega$).

scheme. This is equivalent to find out the minimum of $\rho(M)$ for $\rho(G) > \sqrt{\omega - 1}$. Using equation (9), it is simple to prove that the following inequality has to hold true for $|\ell| < 1$:

$$\sqrt{\omega - 1} \leq \max\left(|\lambda^{+}(\ell)|, |\lambda^{-}(\ell)| \right), \tag{A.13}$$

and the equal sign holds true when $\lambda^{\pm}(\ell) \in \mathbb{C}$. This is schematically sketched in Fig. A.1. This means that the maximum convergence rate is achieved when the eigenvalue of M with the maximum absolute value is complex, that is for $\rho(G) \leq 2\sqrt{\omega - 1}/\omega$. Then, summarizing, we require:

$$\sqrt{\omega - 1} < \rho(G) \leq \frac{2}{\omega}\sqrt{\omega - 1}. \tag{A.14}$$

In this range, $\rho(M) = \sqrt{\omega - 1}$ and the above relation can be rewritten as follows:

$$\rho(M) < \rho(G) \leq \frac{2}{\omega}\sqrt{\omega - 1}. \tag{A.15}$$

Consequently, the optimal action of the DOR scheme is achieved when $\rho(G)$ equals the upper bound, that is $\rho(G) = 2\sqrt{\omega - 1}/\omega$. Solving this equation for ω, we find:

$$\omega = \frac{2}{1 + \sqrt{1 - \rho(G)^2}}. \tag{A.16}$$

This represents the optimal value for the relaxation parameter. □

Appendix B. Basic iterative schemes

The simplest iterative scheme is the Richardson's method. In the context of elliptic partial differential equations, this may be assimilated to a pseudo-compressible approach as follows:

$$\frac{\partial u}{\partial \tau} = a^2 \left(L[u] - b \right), \tag{B.1}$$

where τ represents a pseudo-time and a is a thermal-like diffusivity. In this way, the elliptic equation represented by the system (1) is transformed in a parabolic equation and the solution of the initial problem is achieved as an asymptotic stationary state. The discrete scheme reads:

$$x_{n+1} = x_n + \Delta\tau \left(A\, x_n - b \right). \tag{B.2}$$

The convergence of the scheme is ensured by the fact that the eigenvalues of A are negative and by the choice of the pseudo-time step $\Delta\tau$. Specifically, the scheme is convergent if $0 < \Delta\tau < 2/\rho(A)$ while the optimal choice for $\Delta\tau$ is:

$$\Delta\tau_{opt} = \frac{2}{\rho(A) + |\lambda_m|}, \tag{B.3}$$

where λ_m is the eigenvalue of A with the minimum modulus (see [1] for details). For $\Delta\tau = \Delta\tau_{opt}$, one obtains the minimum spectral radius (i.e. the fastest convergence rate):

$$\rho(G) = \frac{\rho(A) - |\lambda_m|}{\rho(A) + |\lambda_m|}\,. \tag{B.4}$$

We use the optimal pseudo-time step described in (B.3) in all the simulations where reliable approximations of $\rho(A)$ and $|\lambda_m|$ are available. In section B.1, we give a brief overview of the theoretical results concerning the eigenvalues of the discrete Poisson equation.

The Jacobi and Gauss–Seidel methods are obtained through a proper rearrangement of the matrix A. Let us consider the equation (1) and write $A = D - E - F$ where D is the diagonal matrix, $-E$ is the lower triangular matrix and $-F$ is the upper triangular matrix. The Jacobi scheme reads:

$$x_{n+1}^{(J)} = D^{-1}\,(E + F)\,x_n + D^{-1}b\,, \tag{B.5}$$

while the JOR method is derived straightforwardly by applying the over-relaxation step as follows:

$$x_{n+1}^{(JOR)} = \omega\, x_{n+1}^{(J)} + (1-\omega)\,x_n\,. \tag{B.6}$$

A bit more complex is the derivation of the SOR scheme. First, we introduce the Gauss–Seidel method. Following [1], this can be defined as follows:

$$x_{n+1} = D^{-1}\,(E\,x_{n+1} + F\,x_n) + D^{-1}b\,, \tag{B.7}$$

and may be regarded as a modification of equation (B.5). Note that the iteration step described in equation (B.7) is not truly implicit. In fact, since $D^{-1}E$ is a lower triangular matrix, the component $x_{n+1}^{(i)}$ that has been just computed is used to derive the component $x_{n+1}^{(i+1)}$. The global iteration x_{n+1} can be obtained by rearranging the equation (B.7) in the following manner:

$$x_{n+1}^{(GS)} = (D-E)^{-1}\,F\,x_n + (D-E)^{-1}\,b\,. \tag{B.8}$$

This represents the explicit form of the Gauss–Seidel method. The inclusion of the over-relaxation step to obtain the SOR method is slightly different from the procedure adopted for JOR scheme. Indeed, the over-relaxation step is not applied to equation (B.8) but to equation (B.7), leading to:

$$x_{n+1} = \omega\left[\,D^{-1}\,(E\,x_{n+1} + F\,x_n) + D^{-1}b\right] + (1-\omega)\,x_n\,. \tag{B.9}$$

Similarly to equation (B.7), this iteration step is not truly implicit because $\omega D^{-1}E$ is a lower triangular matrix. After some manipulations, we obtain

$$x_{n+1}^{(SOR)} = (D - \omega\,E)^{-1}\,[\,\omega\,F + (1-\omega)\,D\,]\,x_n + \omega\,(D - \omega\,E)^{-1}\,b\,, \tag{B.10}$$

which represents the global iteration x_{n+1} of the SOR method. The optimal choice of ω for JOR and SOR may be quite complex and we address the reader to [1,2] for an in-depth treatise.

B.1. Eigenvalues of the discrete Poisson equation in Cartesian coordinates

Let us consider the Laplace equation in one-dimension and assume to discretize it by finite difference on a uniform Cartesian grid. Then, the maximum and minimum eigenvalues for the Dirichlet problem are:

$$\lambda_{max} = \frac{2}{\Delta x^2}\left[1 - \cos\left(\frac{N\,\pi}{N+1}\right)\right], \quad \lambda_{min} = \frac{2}{\Delta x^2}\left[1 - \cos\left(\frac{\pi}{N+1}\right)\right],$$

where Δx is the spatial step and N indicates the total number of grid points. For large N, we obtain the following limits:

$$\lambda_{max} \to \frac{4}{\Delta x^2}\,, \qquad \lambda_{min} \to \frac{1}{\Delta x^2}\left(\frac{\pi}{N+1}\right)^2 \simeq \left(\frac{\pi}{L}\right)^2\,, \tag{B.11}$$

where L is the length of the computational domain. In the presence of Neumann conditions, the limit of λ_{max} still provides a good approximation for N large. Conversely, $\lambda_{min} = 0$ for every choice of N since the solution of the Laplace equation is defined for less than an inessential constant value. For finite difference schemes, the extension in two and three dimensions is straightforward since the Laplace operator may be split in each Cartesian direction. Consequently, the maximum and minimum eigenvalues are given by the following summations:

$$\lambda_{max} = \lambda_{max}^{(x)} + \lambda_{max}^{(y)} + \lambda_{max}^{(z)}\,, \qquad \lambda_{min} = \lambda_{min}^{(x)} + \lambda_{min}^{(y)} + \lambda_{min}^{(z)}\,,$$

where the superscript indicates the Cartesian direction along which the eigenvalue has been evaluated.

Appendix C. MR-DOR method: details of computation

Applying the matrix A to each equation of the system (20), we find:

$$\begin{cases} r^*_{n+1} = r_n + \Delta\tau\, A\, r_n\,, \\ r_{n+1} = \omega\, r^*_{n+1} + (1-\omega)\, r_{n-1}\,, \end{cases} \tag{C.1}$$

where r_n indicates the residue at the n-th iteration (namely, $r_n = A\,x_n - b$).

We first focus on the definition of the parameter ω_n. From the second equation of system (C.1), we compute the square norm of the residue r_{n+1}:

$$\|r_{n+1}\|^2 = \omega^2\, \|r^*_{n+1}\|^2 + 2\,\omega\,(1-\omega)\,\langle\, r_{n-1},\, r^*_{n+1}\,\rangle + (1-\omega)^2\, \|r_{n-1}\|^2\,,$$

and rearrange it as follows:

$$\|r_{n+1}\|^2 = \omega^2\, \|r_{n-1} - r^*_{n+1}\|^2 + 2\,\omega\,\left(\langle\, r_{n-1},\, r^*_{n+1}\,\rangle - \|r_{n-1}\|^2\right) + \|r_{n-1}\|^2\,.$$

This represents a parabola with convex profile in the variable ω. As a consequence, $\|r_{n+1}\|^2$ admits a unique local (and global) minimum at the point ω_n that satisfies:

$$\frac{\mathrm{d}\|r_{n+1}\|^2}{\mathrm{d}\omega} = 2\,\omega\, \|r_{n-1} - r^*_{n+1}\|^2 + 2\,\left(\langle\, r_{n-1},\, r^*_{n+1}\,\rangle - \|r_{n-1}\|^2\right) = 0\,.$$

Solving the above equation, we obtain:

$$\omega_n = \frac{\langle\, r_{n-1},\, r_{n-1} - r^*_{n+1}\,\rangle}{\|r_{n-1} - r^*_{n+1}\|^2}\,. \tag{C.2}$$

For what concerns $\Delta\tau_n$, this is obtained by imposing the minimization of $\|r^*_{n+1}\|^2$. In this case, we focus on the first equation of system (C.1) and, following the same procedure described above for ω_n, we find:

$$\Delta\tau_n = -\,\frac{\langle r_n\,,\, A\, r_n\rangle}{\|A\, r_n\|^2}\,. \tag{C.3}$$

If A is negative definite, $\Delta\tau_n$ is always positive.

References

[1] A. Quarteroni, A. Valli, Numerical Approximation of Partial Differential Equations, Springer-Verlag, 1994.
[2] Y. Saad, Iterative Methods for Sparse Linear Systems, second edition, Society for Industrial and Applied Mathematics (SIAM), 2003.
[3] M. Dehghan, M. Hajarian, Improving preconditioned SOR-type iterative methods for L-matrices, Int. J. Numer. Methods Biomed. Eng. 27 (5) (2011) 774–784.
[4] M. Dehghan, M. Dehghani-Madiseha, M. Hajarian, A generalized preconditioned MHSS method for a class of complex symmetric linear systems, Math. Model. Anal. 18 (4) (2013) 561–576.
[5] H. Moghaderi, M. Dehghan, A multigrid compact finite difference method for solving the one-dimensional nonlinear sine-Gordon equation, Math. Methods Appl. Sci. 38 (17) (2015) 3901–3922.
[6] A. Pletzer, B. Jamroz, R. Crockett, S. Sides, Compact cell-centered discretization stencils at fine-coarse block structured grid interfaces, J. Comput. Phys. 260 (2014) 25–36.
[7] J. Huang, L. Greengard, A fast direct solver for elliptic partial differential equations on adaptively refined meshes, SIAM J. Sci. Comput. 21 (2000) 1551–1566.
[8] G.I. Taylor, A.E. Green, Mechanism of the production of small eddies from large ones, Proc. R. Soc. Lond. Ser. A 158 (1937) 499–521.
[9] Xiyang I.A. Yang, Rajat Mittal, Acceleration of the Jacobi iterative method by factors exceeding 100 using scheduled relaxation, J. Comput. Phys. 274 (2014) 695–708.
[10] Ming-Chih Lai, A note on finite difference discretizations for Poisson equation on a disk, Numer. Methods Partial Differ. Equ. 17 (3) (2001) 199–203.